Biosensors and Bioelectronics 29 (2011) 82–88

Contents lists available at ScienceDirect

Biosensors and Bioelectronics

journal homepage: www.elsevier.com/locate/bios

Immobilization of rat brain acetylcholinesterase on ZnS and poly(indole-5-carboxylic acid) modified Au electrode for detection of organophosphorus insecticides

Nidhi Chauhan, Jagriti Narang, C.S. Pundir*

Department of Biochemistry, M. D. University, Rohtak 124 001, Haryana, India

ARTICLE INFO

Article history:
Received 5 June 2011
Received in revised form 13 July 2011
Accepted 27 July 2011
Available online 3 August 2011

Keywords:
Acetylcholinesterase
ZnS nanoparticles
Poly(indole-5-carboxylic acid)
Organophosphorus compounds
Amperometric biosensor

ABSTRACT

A novel, highly sensitive amperometric biosensor for detection of organophosphorus (OP) compounds has been constructed, based on rat brain acetylcholinesterase (AChE) immobilized onto nanocomposite of ZnS-nanoparticles (ZnSNPs) and poly(indole-5-carboxylic acid) electrodeposited on Au electrode. In the presence of acetylthiocholine chloride (ATCl) as a substrate, ZnSNPs promoted electron transfer reactions at a lower potential and catalyzed electrochemical oxidation of enzymatically formed thiocholine, thus increasing detection sensitivity. Under optimum conditions (phosphate buffer, pH 7.5 and 30 °C), the inhibition of AChE by malathion and chlorpyrifos was proportional to their concentrations in the range, 0.1–50 nM and 1.5–40 nM, respectively. The biosensor determined malathion and chlorpyrifos in spiked tap water samples with a acceptable accuracy (95–100%). The enzyme electrode had long-storage stability (50% retention of initial activity within 2 months, when stored at 4 °C).

1. Introduction

Acetylcholinesterase (AChE) (acetylcholine acetylhydrolase; EC 3.1.1.7) has attracted the attention of several workers, as it is inhibited significantly by organophosphorus (OP) compounds, used in medicine, agriculture, industry and as chemical warfare agents (Shi et al., 2006). The enzyme inhibition mechanism proceeds through the formation of a stable complex through reversible/irreversible reaction of OP pesticides with the active site of AChE (Neufeld et al., 2000). As a result, acetylcholine, a neurotransmitter is accumulated, due to reduced activity of AChE and causes the nerve order to be reiterated, leading to exhaustion and paralysis. This ultimately corroborates the need for the detection of OP pesticides in the environment. During the past, OP pesticides have been effectively monitored using various chromatographic techniques (Corcia and Marchetti, 1991) such as gas chromatography (GC), high performance liquid chromatography (HPLC) (Sherma, 1993) and thin layer chromatography (TLC) (Linford, 1990). Although these chromatographic techniques provide fruitful results, these are rather time consuming and need very expensive equipment, highly trained personnel beside complicated sample preparation.

As highly sensitive and highly selective tools, biosensors can be used as disposable sensors in environmental monitoring and thus overcome the shortcomings of the conventional chromatographic methods for OP determination (Rogers and Gerlach, 1996). In recent years, the use of nanomaterials in AChE biosensors has resulted into their improved analytic performance, such as CdS nanoparticles (Pardo-Yissar et al., 2003), ZrO_2/chitosan composite film (Yang et al., 2005), multiwalled carbon nanotubes (MWCNTs) (Liu and Lin, 2006), Prussian blue (PB) (Arduini et al., 2006; Sun and Wang, 2010), gold–platinum bimetallic nanoparticles (Upadhyay et al., 2009), one-dimensional gold nanoparticles (YanRong et al., 2010), ionic liquid–multiwalled carbon nanotube (IL–MWCNT) (Rotariu et al., 2010), 1-butyl-3-methylimidazolium tetrafluoroborate/multiwalled carbon nanotube composite gel (Zamfir et al., 2011), nanostructured films of acetylcholinesterase and CdTe quantum dots (Zheng et al., 2011) and MWCNTs, gold nanoparticles (GNPs) and PB (Sun et al., 2011). However, all these biosensor had some common drawbacks such as low sensitivity, low storage stability and reusability. ZnS nano materials are chemically more stable and technologically better than other chalcogenides (such as ZnSe). These nanomaterials are considered to be a promising host material due to their excellent prospective in catalysis owing to their quantum size and magnetic functionality (Peng et al., 2006).

Among various conducting polymers used for immobilization of enzymes, such as polyacetylene, polythiophene, polypyrrole and polyaniline, polyindole (Pin) is better polymer, as it can be easily polymerized, with ease of membrane formation and has high conductivity and chemical stability (Periasamy et al., 2009). Further,

* Corresponding author. Tel.: +91 9416492413; fax: +91 126274640.
E-mail addresses: pundircs@rediffmail.com, pundircs@gmail.com (C.S. Pundir).

0956-5663/$ – see front matter © 2011 Elsevier B.V. All rights reserved.
doi:10.1016/j.bios.2011.07.070

the polyindole films have fairly good thermal stability, high redox activity and slow degradation rate in comparison with polypyrrole and polyaniline (Diehl-Faxon et al., 1996; Billaud et al., 1995). The present report describes the use of nanocomposite of Pin5COOH and ZnSNPs to promote the electron transfer and thus increase the detection sensitivity of an AChE biosensor.

2. Experimental

2.1. Chemical and reagents

Acetylthiocholine chloride, indole-5-carboxylic acid, acetonitrile and 2-pyridine aldoxime methiodide [2-PAM] from Sigma–Aldrich Chemical Co. USA were used. α-Methyl-D-mannoside, Triton X-100, 5,5′-dithiobis(2-nitrobenzoic acid) (DTNB), zinc acetate and sodium sulphide, $K_3Fe(CN)_6$, $K_4Fe(CN)_6$, $FeCl_3$, NaCl, KCl, sodium phosphate, *N*-ethyl-*N*′-(3-dimethylaminopropyl) carbodiimide (EDC) and *N*-hydroxysuccinimide (NHS) were from Sisco Research Laboratory, Mumbai. The pesticides (malathion and chlorpyrifos) were from Lentrek North America (San Francisco, CA). Gold wire (1.5 cm × 0.05 cm) (23 carat) was purchased from local market. All other chemicals were of analytical reagent (AR) grade. Double distilled water (DW) was used throughout the experiments.

2.2. Preparation of rat brain acetylcholinesterase

We have purified a membrane-bound AChE from adult rat brain because of its high specific activity compared to commercially available enzymes (Wenthold et al., 1974; Nunes et al., 2001). All operations were carried out at 4 °C. The brains of 7 adult rats (6.7 g) were homogenized in 60 ml of saline buffer (12.5 mM sodium phosphate buffer, pH 7.2 containing 0.4 M NaC1) in a glass homogenizer with Teflon pestle and the suspension was centrifuged at 25,000 × *g* for 2 h. The supernatant was discarded and the pellet was suspended into 60 ml of distilled water. The suspension was added slowly to 100 ml of saline buffer (13.75 mM phosphate buffer, pH 7.2 containing 0.44 M NaCl and 0.55% Triton X-100) and stirred for 30 min. The suspension was then centrifuged as above. The pellet was discarded and the supernatant treated as crude enzyme (Rakonczay et al., 1981). It was tested for AChE activity as described by Ellman et al. (1961) with modification and protein as described by Lowry et al. (1951) method. The enzyme was purified by gel filtration on Sephadex G-100 column (40 cm × 2 cm) using 13.75 mM sodium phosphate buffer pH 7.2 containing 0.5 M α-methyl-D-mannoside and ion exchange chromatography on DEAE-Sephacel column (16 cm × 1 cm) using a linear gradient of KCl (0.1–0.6 M) Tris–HCl buffer pH 8.5 for elution of enzyme. The purified enzyme was dialysed against 0.05% Triton X-100 and stored at −20 °C.

2.3. Assay of acetylcholinesterase

AChE preparation (100 μl containing 2.7 U, 1.07 μg protein) was added to 150 μl of DW. After pre-incubation for 10 min at 30 °C, 250 μl of 12.5 mM acetylthiocholine chloride in 100 mM sodium phosphate buffer, pH 7.0, was added to diluted enzyme and incubated further for 120 min at 30 °C. After incubation, 500 μl of the reaction mixture was transferred to a new vial, and then 1375 μl of 100 mM sodium phosphate buffer, pH 7.0 and 75 μl of DTNB in 100 mM sodium phosphate, pH 7.0, was added to this vial. A_{412} was read in a UV-Spectrophotometer (Shimadzu, model 1700) after 1 min. The control was run in the same manner as described above except that the enzyme was replaced by DW. The following chemical reaction occurred during the assay of enzyme:

$$\text{Acetylthiocholine chloride} + H_2O \xrightarrow{\text{AChE}} \text{Thiocholine} + \text{Acetic acid}$$

$$\text{Thiocholine} + \text{DTNB} \xrightarrow{\text{AChE}} \underset{\text{Yellow colour}\,(\lambda_{max}=412)}{\text{Thionitrobenzoic acid}}$$

$$+\text{Thionitrobenzoic acid} - \text{Thiocholine}$$

One enzyme unit is defined as 1 μmol of thiol group appearance/min/ml. The enzyme activity was calculated using the following formula:

$$R = \frac{\Delta A}{1.36 \times 10^4} \times \frac{1}{(250/1950)C_o} = 5.74 \times 10^{-4} \frac{\Delta A}{C_o},$$

where R is the rate, in moles substrate hydrolyzed per min per ml of enzyme; ΔA is the change in absorbance at 412 nm per min; C_o is the original concentration of enzyme in solution (mg protein/ml); 1.36×10^4 is the extinction coefficient of DTNB; 1950 refers to 1950 μl total volume of reaction mixture; 250 refers to 250 μl enzyme added.

2.4. Preparation of zinc sulphide (ZnS) nanoparticles

Zinc sulphide (ZnS) nanoparticles were synthesized by chemical precipitation method of Sharma et al. (2008). Aqueous solutions of 0.5 M zinc acetate ($Zn(CH_3COO)_2{\cdot}H_2O$) and 0.5 M sodium sulphide (Na_2S) were used for synthesis of ZnS nanoparticles. To 100 ml zinc acetate (0.5 M), sodium sulphide (0.5 M) was added drop-wise under constant stirring until white coloured precipitates appeared. The stirring was allowed further for 15 min at room temperature. The precipitated particles were filtered using Whatman No. 40 filter paper. To remove the last traces of adhered impurities, the particles were washed several times with DW. The washed particles were dried at 60 °C in air.

2.5. Preparation of ZnS/Pin5COOH nanocomposites

It was prepared as described (Vu et al., 2005) with modification. Firstly, dispersion was prepared by mixing of 10.0 g ZnSNP and 1.0 ml indole monomers in 50.0 ml distilled water. Then 4.5 g $FeCl_3$ (as oxidizing agent for polyindole synthesis) was added to the ZnS particle dispersion during stirring. After 2 h of stirring, the particles were cleaned by DW, filtered, extracted for 10 h and dried at 50 °C.

2.6. Construction of nanocomposites modified Au electrode

Electropolymerization of nanocomposite was carried out on Au electrode (1.5 cm × 0.05 cm) from acetonitrile solution containing ZnS/Pin5COOH nanocomposite (Biegunski et al., 2006). Before electropolymerization, the Au electrode was polished with alumina powder (diameter 0.05 μm) followed by ultrasonic cleaning with DW. For polymer nanocomposite film formation, the electropolymerization was achieved by immersing Au electrode in a solution (25 ml, phosphate buffer pH 7.5) containing 0.1 g nanocomposite and then applying 10 polymerization cycles in the potential range from 0.0 V to +0.6 V and back to 0.0 V at a sweep rate of 20 mV s^{-1}. After polymerization the electrode was washed carefully with a mixture of acetonitrile and DW (1:1 ratio) and finally with DW. On such prepared surface, few drop of enzyme solution were added and then 0.1 ml mixture of 0.2 M EDC and 0.2 M NHS in 1:1 ratio (adjusted pH 6.0) was also added. After 10 min, the electrode was washed with DW and used for measurements (Scheme 1A).

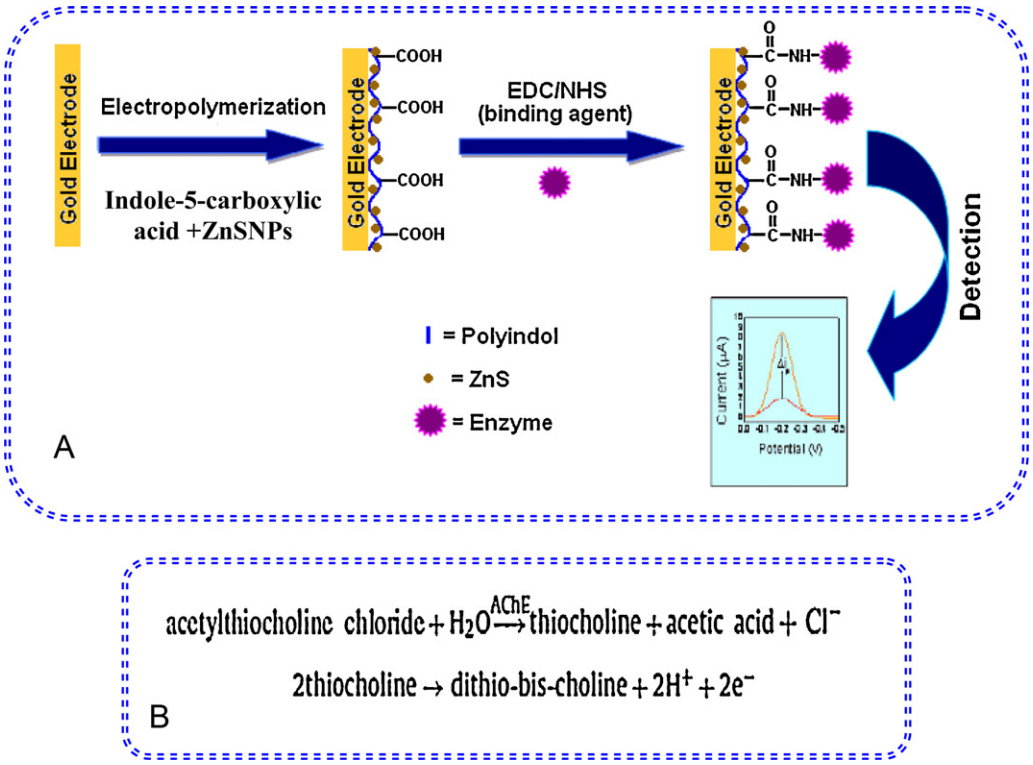

Scheme 1. (A) Schematic illustration of the stepwise amperometric biosensor fabrication process and immobilization of enzyme. (B) Measurement of electrochemical response.

2.7. Electrochemical measurement

Electrochemical measurements were carried out in a Potentiostat/Galvanostat (Autolab, Eco Chemie, The Netherland. Model: AUT83785 with General Purpose Electrochemical System (GPES), software, version 4.9) with a three electrode system consist of a Pt wire as an auxiliary electrode, an Ag/AgCl electrode as reference electrode and modified Au wire as a working electrode. The three-electrode system was pre-equilibrated at +0.2 V for 15 s before each run of detection and the steady current readings were obtained at +0.2 V (vs. Ag/AgCl). After 100 μl of ATCl (15 mg ml^{-1}) solution was injected into the cell containing 10 ml phosphate buffer (0.1 M, 7.0), a low voltage of +0.2 V was applied. The substrate (ATCl) was enzymatically hydrolyzed to thiocholine, which was then subjected to electrocatalytic oxidative dimerisation at +0.2 V vs. Ag/AgCl to generate the disulphide compound. This response, due to the oxidation of the thiocholine at the working electrode, was correlated to the activity of AChE (Scheme 1B).

2.8. Analytical procedure

2.8.1. Inhibition by pesticides

For measurement of malathion, the AChE-Pin5COOH/ZnS/AuE was first immersed in the buffer solution (pH 7.5) containing different concentrations of standard malathion or samples for 12 min, and then transferred to the electrochemical cell of 10.0 ml, 0.1 M phosphate buffer pH 7.5 containing 0.5 mM ATCl to measure the electrochemical response of biosensor. The inhibition by malathion was calculated as follows:

$$\text{Inhibition}\,(\%) = 100 \times \frac{i_{\text{p,control}} - i_{\text{p,exp}}}{i_{\text{p,control}}},$$

where $i_{\text{p,control}}$ is the peak current of ATCl on AChE-Pin5COOH/ZnS/AuE; $i_{\text{p,exp}}$ is the peak current of ATCl on AChE-Pin5COOH/ZnS/AuE with malathion inhibition.

2.8.2. Enzyme reactivation

After AChE-Pin5COOH/ZnS/AuE was exposed to pesticides, it was washed with phosphate buffer (pH 7.0) and reactivated by dipping it into 2 ml of 4.0 mM 2-pyridine aldoxime methiodide [2-PAM] in 0.1 M phosphate buffer pH 7.0 for 5–20 min, then transferred to electrochemical cell containing 10 ml of reaction buffer pH 7.5 consisting 0.5 mM ATCl to study the electrochemical response. The reactivation efficiency (R%) was estimated as follows:

$$R(\%) = 100 \times \frac{i_{\text{r}} - i_{\text{p,exp}}}{i_{\text{p,control}} - i_{\text{p,exp}}},$$

where i_{r} is the peak current of ATCl on AChE-Pin5COOH/ZnS/AuE with 2-pyridine aldoxime methiodide [2-PAM] reactivation.

2.9. Stability and reproducibility of the biosensor

To reuse the working electrode, it was washed by dipping it in 10 ml of 0.1 M phosphate buffer pH 7.5. The long-term storage and stability of the biosensor was investigated over 2 months, when AChE-Pin5COOH/ZnS/AuE was stored dry in a refrigerator at 4 °C. AChE-Pin5COOH/ZnS/AuE activity was measured once in a week.

3. Results and discussions

The yield of the purified rat brain AChE (specific activity: 2507 U/mg protein) was 51%.

3.1. TEM image and XRD pattern of ZnS nanoparticles and UV/Vis spectra of nanocomposites

The morphological characterization of nanoparticles was carried out by Transmission Electron Microscope (TEM) at Department of Anatomy, AIIMS, New Delhi. TEM of ZnS nanoparticles as shown in Fig. 1A revealed that ZnS were very fine with diameter in the range 13–58 nm. The XRD pattern of synthesized ZnS powder as

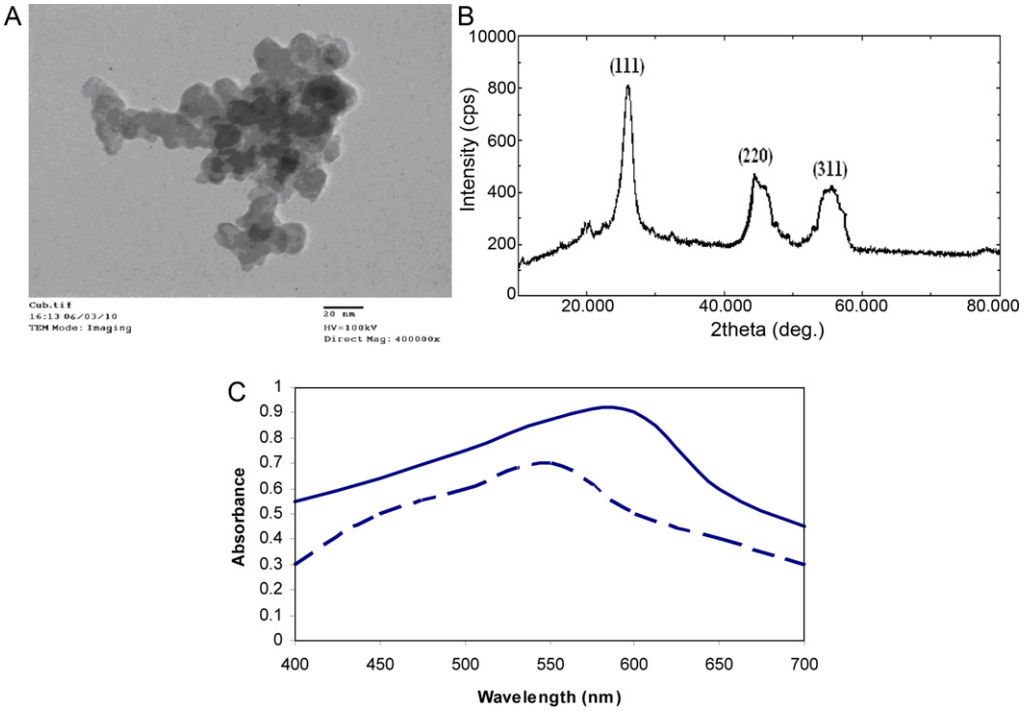

Fig. 1. (A) Transmission electron microscope (TEM) image of ZnS nanoparticles and (B) X-ray diffraction (XRD) pattern of ZnS nanoparticles. (C) Changes in the UV/Vis spectra of ZnS nanoparticles before (. . . . .) and after the addition of indole (——).

given in Fig. 1B, showed three broad peaks corresponding to the (111), (220) and (311) planes. Crystallite size of ZnS nanoparticles was calculated by following Scherrer's equation,

$$D = \frac{\kappa\lambda}{\beta \cos\theta}, \quad (1)$$

where $k = 0.9$, D is the crystallite size (Å), λ(Å) = 1.54 be the wavelength of Cu Kα radiation and β is the corrected half width of the diffraction peak. The average crystallite size calculated from these peaks using Scherer's formula was 2 nm. Three peaks were observed in the span ranging from 5° to 100°. The peaks observed in the XRD patterns matched well with earlier reported literature (Sharma et al., 2008). Intensities of the three most important peaks of ZnS, namely ⟨1 1 1⟩, ⟨2 2 0⟩ and ⟨3 1 1⟩ reflections were corresponding to 28.5°, 47.6° and 56.4° respectively. Broadening of the XRD peaks indicated the formation of ZnS nanocrystals.

Fig. 1C shows the UV/Vis spectra recorded in UV-Vis spectrophotometer for ZnS nanoparticles before and after the addition of 1.0 ml indole monomers in 50.0 ml distilled water. Then 4.5 g $FeCl_3$ was added to the ZnS particle dispersion during stirring. After 2 h of stirring, the particles were cleaned by distilled water, filtered, extracted for 10 h. The aggregation of ZnS nanoparticles with polyindole (Pin5COOH) shifted the absorption band to longer wavelength.

3.2. Morphology of nanocomposites modified electrode

Fig. 2A–C shows the typical scanning electron micrograph of bare AuE, Pin5COOH/ZnS/AuE and AChE-Pin5COOH/ZnS/AuE. The nanocomposite and enzyme mixture were prepared on the Au electrode via the one-step carbodiimide linkage between enzyme and nanocomposite. To investigate the microstructure of Pin5COOH/ZnS/AuE, the morphology of Pin5COOH/ZnS film was examined by SEM as shown in Fig. 2B. Fig. 2C shows that the enzyme was chemically immobilized in the nanocomposites structure and formed a regular array on the surface of the Au electrode.

3.3. Evidence of enzyme immobilization

Fig. 3A shows the cyclic voltammograms of bare Au electrode (a), Pin5COOH/ZnS modified Au electrode (b) and AChE immobilized onto Pin5COOH/ZnS modified Au electrode (c) in the presence of 0.5 mM ATCl in phosphate buffer (0.1 M, pH 7.5). No peak was observed in case of unmodified electrode, while cyclic voltammograms (CV) obtained during electropolymerization of nanocomposite in acetonitrile solution. The polymer exhibited two characteristic redox processes in acetonitrile solution, whereas no detectable signal was observed without immobilization of enzyme. The first process is taking place at +0.15 V. It is believed that this process could be ascribed to the creation of radical cations and the formation of a very stable polycationic intermediate form (Billaud et al., 2003). The second process takes place at +0.57 V, so it coincides with the oxidation of monomer. This process, accompanied by deprotonation of the intermediate state, leads to a fully oxidized polymer form. The polymeric films were produced by applying 4 deposition cycles. Barlett et al. (1992) showed that the polymer was stable, conducting and electroactive in aqueous solution in the broad pH range. Nanocomposite provided a conductive path for electron transfer and promoted electron transfer reactions at a lower potential. On such prepared surface, when few drops of enzyme solution were added followed by addition of mixture of EDC/NHS reagent, it resulted into immobilization of enzyme on the polymer surface, which was revealed by a decrease of anodic and cathodic currents.

To confirm enzyme immobilization on the Pin5COOH film the FTIR spectra was recorded in FTIR spectrometer (Make: iS10, Thermoelectron, USA). Fig. 3B shows FTIR spectra for Pin5COOH/ZnS/Au electrode (curve i) and AChE-Pin5COOH/ZnS/Au electrode (curve ii). The spectrum associated with the oxidized Pin are characterized by a very large adsorption band located in the spectral domain between 3700 and 3100 cm^{-1}, which is a characteristic of –OH groups belonging to residual water molecules trapped in the polymer matrix as well as water molecules absorbed in Pin. The peaks at 3401, 2924, 1593, and 1312 cm^{-1} could be attributed to

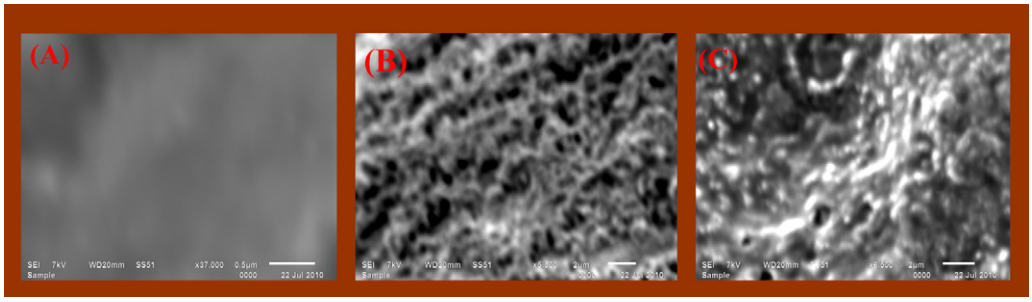

Fig. 2. Scanning electron microscopy (SEM) image of (A) bare Au electrode, (B) Pin5COOH/ZnS/AuE and (C) AChE-Pin5COOH/ZnS/AuE.

–N–H stretching, –C–H (aromatic) stretching, C=C stretching and C–N stretching (between two indole units), respectively. A sharp absorption peak was found at 1690 cm^{-1}, which might be due to the attachment of –COOH group onto the indole. In the FTIR spectrum of AChE-Pin5COOH/ZnS/Au electrode (curve ii), AChE binding is indicated by the appearance of additional absorption bands at 1641 and 1539 cm^{-1} assigned to the carbonyl stretch (amide I band) and –N–H bending (amide II band), respectively.

3.4. Impedance measurements

EIS study was carried out to characterize the modified electrode surface. In a typical Nyquist plot, the semicircle portion corresponds to the charge–transfer resistance (R_{ct}) at higher frequency range, while a linear part at lower frequency range represents the diffusion limited process. In this report, EIS study of the modified electrodes was carried out in 1.0 mM $Fe(CN)_6^{3-/4-}$ containing phosphate buffer (pH 7.5) with a frequency range of 0.01 Hz–10 kHz. Fig. 4A, curve (a) showed a very low R_{ct} (230 Ω) at AuE. After modification with Pin5COOH/ZnS, the EIS of the resulting layer showed semicircle domain with an R_{ct} of 1350 Ω (curve b) suggesting that Pin5COOH/ZnS layer blocked the redox probe to diffuse towards the electrode surface. The R_{ct} value increased for the enzyme modified electrode up to 1800 Ω as shown in curve c. This increase in R_{ct} is attributed to the fact that most biological molecules, including enzymes, are poor electrical conductors at low frequencies (at least <10 kHz) and cause hindrance to the electron transfer. These results were supported by the cyclic voltammogram study (Fig. 3A).

3.5. Electrochemical behavior of the AChE-PinCOOH/ZnS modified Au electrode

Fig. S1 (Supplementary data) shows the produced oxidation–reduction peak of 0.5 mM ATCl on AChE-PinCOOH/ZnS modified Au electrode decreasing drastically (curve b) compared with that of the without malathion (curve a) after the electrode was immersed in standard solutions of malathion (5 μg/ml) for 10 min. This is because the insecticide exhibits fairly high acute

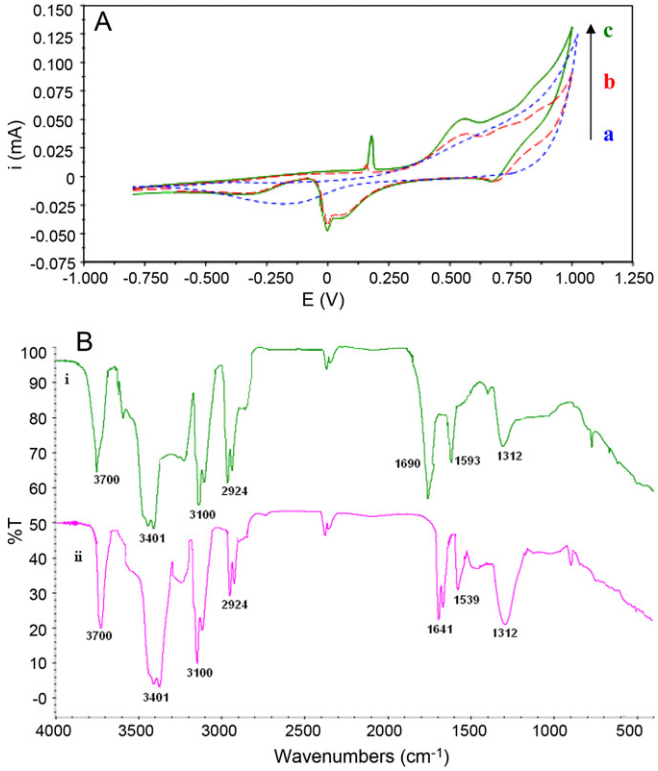

Fig. 3. (A) Cyclic voltammogram (CV) of the bare Au electrode (a), Pin5COOH/ZnS modified Au electrode (b) and AChE immobilized onto Pin5COOH/ZnS modified Au electrode (c) in 0.1 M pH 7.5 phosphate buffer solution at a scan rate of 50 mV s^{-1}. (B) FT-IR spectra of Pin5COOH/ZnS/Au electrode (i) and AChE-Pin5COOH/ZnS/Au electrode (ii).

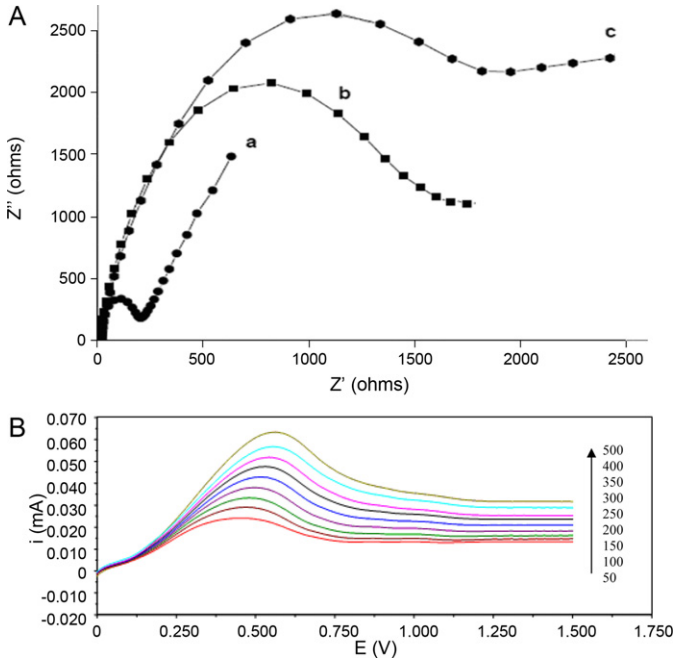

Fig. 4. (A) Electrochemical impedance Nyquist plot of bare AuE (a), Pin5COOH/ZnS/AuE (b) and AChE-Pin5COOH/ZnS/AuE (c) at 0.1 M phosphate buffer containing 0.1 M acetonitrile. Frequency range: 0.01 Hz to 10 kHz. (B) SWV net current responses of biosensor in 0.1 M phosphate buffer (pH 7.5) containing different concentrations (nM) of acetylthiocholine chloride (ATCl) (frequency = 1–100 Hz, potential amplitude = 20 mV).

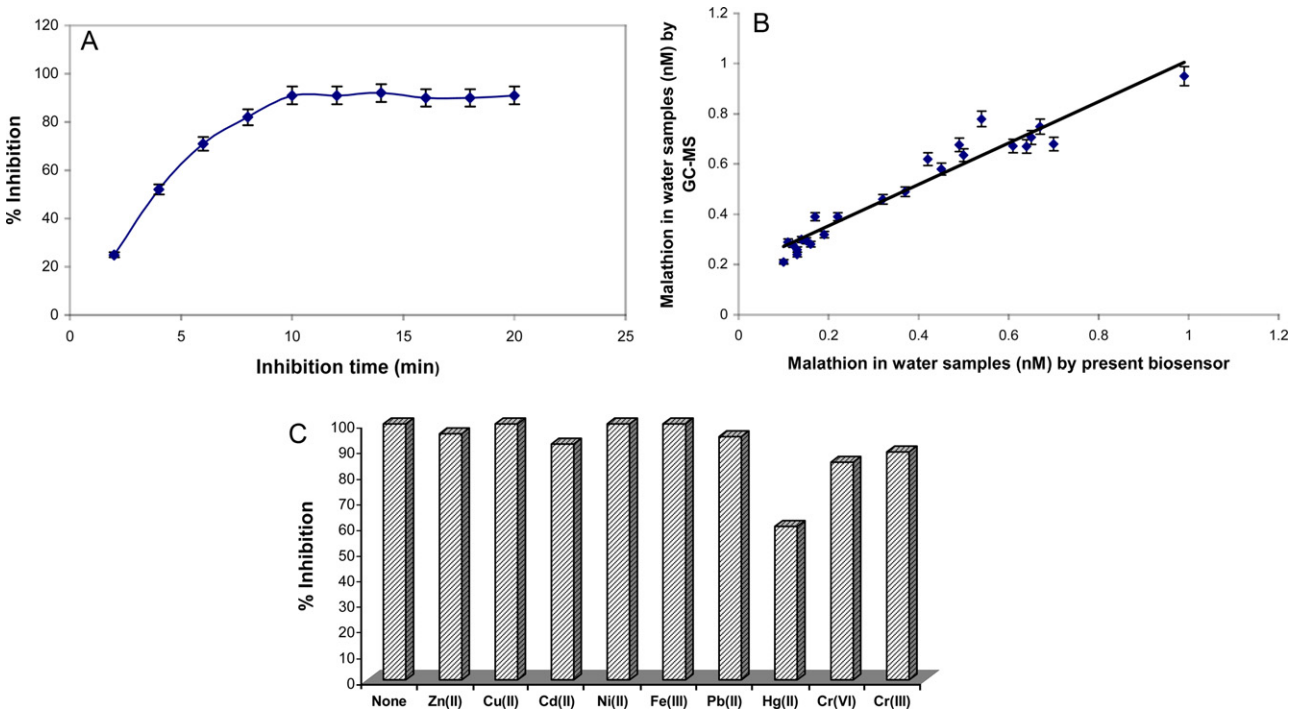

Fig. 5. (A) Effect of inhibition time on malathion inhibition after immersion of the AChE-Pin5COOH/ZnS/AuE in the 5 μg/ml malathion solution. Applied potential +0.2 V vs. Ag/AgCl. (B) Correlation between malathion level in water sample as determined by the present biosensor (*x*-axis) and by the GC–MS method (*y*-axis) based on AChE-Pin5COOH/ZnS/Au electrode. (C) Percent inhibition caused by different metals (each at 2 μM). E_{ap} = +0.2 V vs. Ag/AgCl, phosphate buffer pH 7.5 and acetylthiocholine chloride (ATCl) concentration 0.5 mM.

toxicity and is involved in the irreversible inhibition of AChE, thus reduce the activity of the enzyme to its substrate.

3.6. Optimization of experimental variables

The pH dependence of the biosensor response in 0.1 M phosphate buffer in the pH range of 5.0–8.0 was studied. The response current changed slightly between pH 5.0 and pH 7.0 but the maximum current was observed at pH 7.5. However, the enzyme lost activity irreversibly at the lower or higher pH values. Therefore, 0.1 M phosphate buffer, pH 7.5 was selected as the electrolyte in subsequent experiments. The effect of the temperature on the biosensor response from 20 to 50 °C was also investigated. No significant change in current response was observed during this temperature range except increased slightly at 30 °C. The microenvironment provided by nanocomposite around the enzyme makes it thermally stable and protects it from denaturation and stabilizes its biological activity to a great level. Hence, the optimum temperature (30 °C) was selected for subsequent experiments. The dependence of the biosensor on the applied potential for amperometric signal was also observed. Fig. 4B shows SWV current responses against concentrations of ATCl. Voltammetric measurements were performed after each addition of the ATCl up to a maximum concentration of 0.5 mM. SWV peak currents were found to increase with the concentration of ATCl from 0.005 to 0.5 mM. A good linear relationship of response current with substrate concentration from 0.005 to 0.5 mM is evident from SWV studies. The optimum substrate concentration was 0.5 mM.

3.7. Linear working range and detection limit

The detection limit and the linear working range of the biosensor were evaluated for both pesticides using SWV. There was a linear relationship between current vs. concentration of the inhibitor (OP pesticides) in the range 0.1–50 nM for malathion and 1.5–40 nM for chlorpyrifos. Thus malathion had a wider linear working range compared to chlorpyrifos. Although biosensor was found to be effective for the detection of both the pesticides, it was more sensitive to malathion. The limit of detection of the present biosensor was calculated as the lowest quantity of pesticides required to give a signal to a background (blank) +3 times SD of blank and found to be 0.1 nM for malathion and 1.5 nM for chlorpyrifos.

A comparison of analytic parameters of various nanoparticles based AChE biosensors for detection of pesticides with the present biosensor is summarized in Supplementary Table.

3.8. Effect of inhibition time on the response of AChE-Pin5COOH/ZnS/AuE

For insecticide analysis, one of the most influential parameters is the inhibition time. With an increase of inhibition time in the malathion solution, the peak current of ATCl on the AChE-Pin5COOH/ZnS/AuE was decreased significantly. When the inhibition time was longer than 10 min, the curve tends to a stable value (Fig. 5A), indicating the binding interaction between malathion and active target groups in the enzyme reached saturation.

3.9. Regeneration of acetylcholinesterase

AChE reactivation has been reported by various groups using oximes (Anitha et al., 2004; Gulla et al., 2002). The activity of the immobilized enzyme of the biosensor is inhibited after use. 2-Pyridine aldoxime (2-PAM) has been used to recover the activity of the inhibited AChE (Sagane et al., 2005; Kuswandi et al., 2008). Our experimental results for % recovery of enzyme activity vs. time for treatment of working electrode with 2-PAM, showed that enzymatic activity recovered by 50% at 5 min and fully (97.9%) at 10 min, after which it was constant (up to 20 min) (Fig. S2).

3.10. Precision and recovery

The repeatability and inter-day precision were less than 14% and the accuracy within 95–100%. This demonstrates that the present method was precise and accurate for determination of acetylthiocholine within the range 0.5–20.0 nM. The analytic recoveries of known amount of malathion and chlorpyrifos in tap water samples/spiked samples under optimum conditions were determined by the present biosensor found to be in the range of 95–105%.

3.11. Validation against GC–MS reference methodology

Malathion concentrations in water samples were determined by the present biosensor as well as by conventional gas chromatography–mass spectrometry (GC–MS) method on commercial basis at M/S Arbro Pharmaceuticals Ltd. (Analytical Division), 4/9, Kirti Nagar, Industrial Area, New Delhi, India. The results of both the methods were matched with each other with a regression coefficient ($r = 0.96$) (Fig. 5B).

3.12. Interference study

Heavy metal ions can inhibit the activity of AChE and disturb OP detection using the AChE based biosensor. However, there is no report on the kind and concentration limit of heavy metal ions, which can disturb OP detection. We examined the effects of heavy metal ions such as Zn(II) (as $ZnSO_4$), Cu(II) (as $CuSO_4$), Cd(II) (as $CdSO_4$), Ni(II) (as $NiSO_4$), Fe(III) (as $FeCl_2$), Pb(II) (as $PbCl_2$), Hg(II) (as $HgCl_2$), Cr(VI) (as K_2CrO_4) and Cr(III) (as $CrCl_3$) each at 2 μM on malathion detection by the present biosensor. The results as shown in Fig. 5C, represents the percentage of inhibition. Hg(II) exhibited 40% effect on inhibition similar to earlier reports (Arduini et al., 2005, 2011), while Cr(VI) showed only 15% effect on inhibition. This inhibition was probably due to reaction of thiocholine and metals but not with active site of enzyme.

3.13. Storage stability and reproducibility of biosensor

The modified electrode lost 50% of its initial current response, when stored at 4 °C for 60 days, which is better than that for earlier biosensors (Supplementary Table). Thus, nanocomposites were very efficient for retaining the activity of immobilized AChE and preventing it from leaking out of the electrode. The fabrication reproducibility of biosensor was estimated for determination of 50 nM malathion at three different electrodes for 10 min. The coefficient of variation was found to be 2.7%, which is acceptable.

4. Conclusion

The use of Pin5COOH/ZnS nanocomposites modified Au electrode has resulted into an improved analytical performance of acetylcholinesterase (AChE) biosensor for detection of OP compounds in terms of low working potential (+0.2 V vs. Ag/AgCl), high sensitivity, wide linear range (0.1–50 nM and 1.5–40 nM for malathion and chlorpyrifos respectively) and low detection limit (0.1 and 1.5 nM). The biosensor could be used for the direct determination of pesticides in real samples e.g. soils extract, vegetables, milk and water.

Appendix A. Supplementary data

Supplementary data associated with this article can be found, in the online version, at doi:10.1016/j.bios.2011.07.070.

References

Anitha, K., Mohan, S.V., Reddy, S.J., 2004. Biosens. Bioelectron. 20, 848–856.
Arduini, F., Majorani, C., Amine, A., Moscone, D., Palleschi, G., 2011. Electrochim. Acta 56, 4209–4215.
Arduini, F., Ricci, F., Bourais, I., Amine, A., Moscone, D., Palleschi, G., 2005. Anal. Lett. 38, 1703–1719.
Arduini, F., Ricci, F., Tuta, C.S., Moscone, D., Amine, A., Palleschi, G., 2006. Anal. Chim. Acta 580, 155–162.
Barlett, P.N., Dawnson, D.H., Farrington, J., 1992. J. Chem. Soc. Faraday Trans. 88, 2685–2695.
Biegunski, A.T., Michota, A., Bukowska, J., Jackowska, K., 2006. Bioelectrochemistry 69, 41–48.
Billaud, D., Humbert, B., Thevenot, L., Thomas, P., Talbi, H., 2003. Spectrochim. Acta A Mol. Spectrosc. 59, 163–168.
Billaud, D., Maarouf, E.B., Hannecart, E., 1995. Synth. Met. 69, 571–572.
Corcia, A.D., Marchetti, M., 1991. Anal. Chem. 63, 580–585.
Diehl-Faxon, J., Ghindilis, A.L., Atanasov, P., Willdns, E., 1996. Sens. Actuators B 36, 448–457.
Ellman, G.L., Courtney, K.D., Andres, J.R.V., Featherstone, R.M., 1961. Biochem. Pharmacol. 7, 88–95.
Gulla, K.C., Gouda, M.D., Thakur, M.S., Karanth, N.G., 2002. Biochim. Biophys. Acta 1597, 133–139.
Kuswandi, B., Fikriyah, C.I., Gani, A.A., 2008. Talanta 74, 613–618.
Linford, R.G. (Ed.), 1990. Electrochemical Science and Technology of Polymers. Elsevier Applied Science, London.
Liu, G., Lin, Y., 2006. Anal. Chem. 78, 835–843.
Lowry, O.H., Rosebrough, N.S., Farr, A.L., Randau, R.J., 1951. J. Biol. Chem. 193, 265–275.
Neufeld, T., Eshkenazi, I., Cohen, E., Rishpon, J., 2000. Biosens. Bioelectron. 15, 323–329.
Nunes, G.S., Montesinos, T., Marques, P.B.O., Fournier, D., Marty, J.-L., 2001. Anal. Chim. Acta 434, 1–8.
Pardo-Yissar, V., Katz, E., Wasserman, J., Willner, I., 2003. J. Am. Chem. Soc. 125, 622–623.
Peng, W.Q., Cong, G.W., Qu, S.C., Wang, Z.G., 2006. Opt. Mater. 29, 313–317.
Periasamy, A.P., Umasankar, Y., Chen, S.M., 2009. Sensors 9, 4034–4055.
Rakonczay, Z., Mallol, J., Schenk, H., Vincendon, G., Zanetta, J.P., 1981. Biochim. Biophys. Acta 657, 243–256.
Rogers, K.R., Gerlach, C.L., 1996. Environ. Sci. Technol. 30, 486A–491A.
Rotariu, L., Zamfir, L.-G., Bala, C., 2010. Sens. Actuators B 150, 73–79.
Sagane, Y., Nakagawa, T., Yamamoto, K., Michikawa, S., Oguri, S., Momonoki, Y.S., 2005. Plant Physiol. 138, 1359–1371.
Sharma, M., Kumara, S., Pandey, O.P., 2008. Digest J. Nanomater. Biostruct. 3, 189–197.
Sherma, J., 1993. Anal. Chem. 65, R40–R54.
Shi, M., Xu, J., Zhang, S., Liu, B., Kong, J., 2006. Talanta 68, 1089–1095.
Sun, X., Wang, X., Zhao, W., Du, S., Li, Q., Han, X., 2011. Comput. Comput. Technol. Agricult. IV: IFIP Adv. Inform. Commun. Technol. 344, 16–24.
Sun, X., Wang, X., 2010. Biosens. Bioelectron. 25, 2611–2614.
Upadhyay, S., Rao, G.R., Sharma, M.K., Bhattacharya, B.K., Rao, V.K., Vijayaraghavan, R., 2009. Biosens. Bioelectron. 25, 832–838.
Vu, Q.T., Pavlik, M., Hebestreit, N., Pfleger, J., Rammelt, U., Plieth, W., 2005. Electrochim. Acta 51, 1117–1124.
Wenthold, R.J., Mahler, H.R., Moore, W.J., 1974. J. Neurochem. 22, 941–943.
Yang, Y., Guo, M., Yang, M., Wang, Z., Shen, G., Yu, R., 2005. Int. J. Environ. Anal. Chem. 85, 163–175.
YanRong, L., ZhiYong, G., YanFen, L., Qian, L., Chun, B.J., ZhiHui, D., Min, H., 2010. Sci. China Chem. 53, 820–825.
Zamfir, L.-G., Rotariua, L., Bala, C., 2011. Biosens. Bioelectron. 26, 3692–3695.
Zheng, Z., Zhou, Y., Li, X., Liu, S., Tang, Z., 2011. Biosens. Bioelectron. 26, 3081–3085.